IEEE Access
Multidisciplinary : Rapid Review : Open Access Journal

Received December 20, 2019, accepted January 7, 2020, date of publication January 17, 2020, date of current version January 28, 2020.

Digital Object Identifier 10.1109/ACCESS.2020.2967676

Gaussian Mixture Model Based Probabilistic Modeling of Images for Medical Image Segmentation

FARHAN RIAZ[1], SAAD REHMAN[1], MUHAMMAD AJMAL[2], REHAN HAFIZ[3], ALI HASSAN[1], NAIF RADI ALJOHANI[4], RAHEEL NAWAZ[5], RUPERT YOUNG[6], AND MIGUEL COIMBRA[7]

[1]Department of Computer and Software Engineering, National University of Sciences and Technology, Islamabad 44000, Pakistan
[2]Department of Computer Science and Mathematics, University of Derby, Derby DE22 1GB, U.K.
[3]Department of Computer Engineering, Information Technology University, Lahore 54000, Pakistan
[4]Information Systems Department, King Abdulaziz University, Jeddah 21589, Saudi Arabia
[5]Department of Computing and Mathematics, Manchester Metropolitan University, Manchester M15 6BH, U.K.
[6]School of Engineering and Informatics, University of Sussex, Brighton BN1 9QT, U.K.
[7]Faculty of Sciences, Instituto de Telecomunicações, University of Porto, 4169-007 Porto, Portugal

Corresponding author: Saad Rehman (saadrehman@ceme.nust.edu.pk)

This work was supported in part by National University of Sciences and Technology, Manchester Metropolitan University.

ABSTRACT In this paper, we propose a novel image segmentation algorithm that is based on the probability distributions of the object and background. It uses the variational level sets formulation with a novel region based term in addition to the edge-based term giving a complementary functional, that can potentially result in a robust segmentation of the images. The main theme of the method is that in most of the medical imaging scenarios, the objects are characterized by some typical characteristics such a color, texture, etc. Consequently, an image can be modeled as a Gaussian mixture of distributions corresponding to the object and background. During the procedure of curve evolution, a novel term is incorporated in the segmentation framework which is based on the maximization of the distance between the GMM corresponding to the object and background. The maximization of this distance using differential calculus potentially leads to the desired segmentation results. The proposed method has been used for segmenting images from three distinct imaging modalities i.e. magnetic resonance imaging (MRI), dermoscopy and chromoendoscopy. Experiments show the effectiveness of the proposed method giving better qualitative and quantitative results when compared with the current state-of-the-art.

INDEX TERMS Gaussian mixture model, level sets, active contours, biomedical engineering.

I. INTRODUCTION

Image segmentation is a non-trivial task in computer vision and medical image analysis. In spite of significant advances in various methods that have been developed for image segmentation, achieving better segmentation results remains a significant challenge in medical imaging. This is mainly because most intended applications for image segmentation such as surveillance, object segmentation, etc. are mainly derived from the image edges. Although good results are obtained in such scenarios, differential features (edges, corners, blobs, etc.) when applied to medical images may not lead to good results mainly due to the organic nature of texture in medical images. These features may lead to significant clues about the relevant objects in the images which are subjected to segmentation. Keeping this in view, most of the research on medical image segmentation is focused on the variants of state-of-the-art segmentation methods tailored for specific imaging modalities (incorporating relevant visual structures). This paper aims to investigate the effects of incorporating prior knowledge in the existing segmentation methods based on active contours.

The associate editor coordinating the review of this manuscript and approving it for publication was Victor Hugo Albuquerque.

A. BACKGROUND

Recently, the segmentation methods based on partial differential equations (PDEs) are being widely investigated in the context of segmentation of medical images [1]. The most significant PDE based segmentation methods are based on active contours [2], which are dynamic fronts that move towards boundaries of objects. The level sets formulation was proposed by Osher et al. [3] and implicitly represents a contour as a level set ϕ of high dimensional space. Level sets have been used to implement active contours for image segmentation scenarios. The basic idea is to represent a contour as a level set function and evolve it according to a PDE scheme.

The evolution of PDE for a level set function can be derived by minimizing an energy functional [3]–[5] that is defined on a level set method. Such types of variational methods, when applied to image segmentation, can be very useful as they can incorporate additional information about the images in the level set functions such as shape information, region characteristics, etc. This gives rise to the detection of accurate boundaries and the proper segregation of the image regions representing distinct information.

The energy functionals in active contours integrate the image characteristics (external energy) and geometric characteristics of the contours (internal energy). Minimization of these functionals is solved as a set of PDEs. The external energy functions play a fundamental role in image segmentation. Efforts have been done in the past to propose external energy functions where most of the methods concerning these functions are divided into the following main categories: *region based methods* [6], [7] and *edge based methods* [2], [8] depending on the methodology of employing image data for the evolution of active contours.

The edge-based methods mainly rely on the edge features in the images. In some specific imaging modalities, the edges may not have the requisite strength for segmentation. Kimmel et al. [9] proposed a level set method that integrates an alignment term for settling the active contours to the object boundaries. This term aims at aligning the normal vector of the zero level set curve to the image gradient. A similar approach was proposed by Riaz et al. [10] using creaseness features for measuring the image gradient. Although more accurate segmentation results have been demonstrated, the methods significantly lack in handling the images in which the gradient related to the object boundaries are not strong. Belaid et al. [11] proposed a phase-based level sets method which calculates phase-based features from the images and aligns them with the contours' normal direction of movement. Given that the phase features are more sensitive to variations, good segmentation results are obtained in the case of images with weaker object boundaries. The downside of the algorithm is that the method calculating the edge maps requires careful tuning of the parameters.

In contrast to the edge-based methods, the region-based methods rely on the properties of image regions. The overall homogeneous properties of the objects and background are often less sensitive to noise and are better captured by the region-based methods. Such methods can perform well even if the strength of the edges is weak [12]–[14]. For example, Ji et al. [15] propose a local region-based active contour image segmentation model which uses the variations in local means and variances of local spatial regions to construct a fitting term. Although good results are obtained, the algorithm requires the existence of well-differentiated regions for correct segmentation which is typically not true for medical images. Zhou et al. [16] propose to combine the effects of edge-based methods and a region-based method in which the edge term is formulated using a fitting term that incorporates a dense vector field and a region-based term that localizes the Chan-Vese external force [17]. The effects of the two models are adjusted using the image gradients. This model does not perform well in the case of intensity inhomogeneities which commonly happens in the case of medical images.

In summary, most of the existing methods are aimed at solving some of the common issues that take place during curve evolution using different variants for calculating the edge features from the images followed by the control of flow of the evolving curves [11], [18]–[22]. Although these methods achieve good segmentation results, there are limitations that mostly come from the lack of incorporation of complementary edge and area-based terms into the mathematical frameworks.

B. CONTRIBUTIONS

Keeping this in view, we aim to devise an external energy term that is based on two distinct strategies, one based on the edge-based features from the images and the other which is based on the regional characteristics of the contour. To cater for the edge-based features, we use the edge indicator function whereas for the region based features, we devise a novel term that is incorporated into the distance regularized level sets formulation to perform segmentation. To do this, the curve fitting is performed by formulating an energy term assuming that a mixture of Gaussians can be used to model an image. A contour is initialized followed by curve evolution which maximizes the distance between the empirical distribution for the object and the background using the Bhattacharya distance. The proposed objective function is mathematically solved using differential calculus and implemented using the finite difference scheme. The proposed term is integrated with the existing level sets scheme proposed by Li et al. [23]. A resulting optimization problem is a hybrid approach that is composed of both the edge features and an area term. We validate the segmentation framework on images from three distinct medical imaging modalities: MRI, dermoscopy, and chromoendoscopy. The experimental results are used to validate the effects of adding a region-based term within the segmentation frameworks.

The paper is organized as follows: Section II outlines the background of level sets (LS) followed by a description of the proposed method (Section III). These are followed by experiments (Section IV and V) followed by conclusions (Section VI).

II. BACKGROUND

A. FORMULATION OF ENERGY TERM

Let us assume that we have an image I that can also be indicated by Ω, that is a combination of two mutually exclusive regions: the object R_O and the background R_B i.e. $\Omega \in \{R_O, R_B\}$ separated by a curve ϕ. After initialization of ϕ, the gradient descent algorithm is used to evolve ϕ to the boundaries of the object that has to be segmented by optimizing an energy functional:

$$\mathcal{J} = \gamma \mathcal{R}(\phi) + \mathcal{E}_{ext}(\phi) \tag{1}$$

where $\mathcal{R}(\phi)$ is the regularization term for level sets and $\mathcal{E}_{ext}(\phi)$ is the external energy term that is dependent on the data of interest. For instance, for an image segmentation application, the external energy term is derived from the image data. The levels sets regularization term is defined as

$$\mathcal{R}(\phi) = \frac{1}{2}\int_{\Omega} (\nabla\phi - 1)^2 d\Omega \tag{2}$$

The external energy term $\mathcal{E}_{ext}$ is defined such that it achieves a minimum when the zero level set contour ϕ is located at the desired position. The purpose of adding the regularization term is not just to impose a smoothing effect and also to impose a signed distance property i.e. $\nabla\phi = 1$.

B. ENERGY MINIMIZATION

The minimization of the energy term $\mathcal{J}$ can be done using the calculus of variations. A standard way to minimize the energy functional is to find the steady-state of the gradient flow equation

$$\frac{\partial\phi}{\partial t} = -\frac{\partial\mathcal{J}}{\partial\phi} \tag{3}$$

where $\partial\mathcal{J}/\partial\phi$ is the Gateaux derivative (first variation) of the functional $\mathcal{J}$. This is an evolution equation of an active contour which is time dependent $\phi(x, t)$ with a spatial variable x in the domain Ω and a temporal variable $t \geq 0$. The evolution of gradient flow starts with an initial contour $\phi(x, 0) = \phi_0$ followed by iterations in the direction $-\partial\mathcal{J}/\partial\phi$ which is the steepest descent direction of the functional $\mathcal{J}(\phi)$

$$\frac{\partial\mathcal{J}}{\partial\phi} = \frac{\partial\mathcal{R}}{\partial\phi} + \frac{\partial\mathcal{E}_{ext}}{\partial\phi} \tag{4}$$

where $\partial\mathcal{R}/\partial\phi$ can be written as [24]:

$$\frac{\partial\mathcal{R}}{\partial\phi} = -\left[\Delta\phi - \nabla.\frac{\nabla\phi}{|\nabla\phi|}\right] \tag{5}$$

$\partial\mathcal{E}_{ext}/\partial\phi$ is the Gateaux derivative of the external energy term with respect to ϕ. The gradient flow of $\mathcal{J}$ can be written as

$$\frac{\partial\phi}{\partial t} = \left[\Delta\phi - \nabla.\frac{\nabla\phi}{|\nabla\phi|}\right] - \frac{\partial\mathcal{E}_{ext}}{\partial\phi} \tag{6}$$

This PDE is the level set evolution equation derived from the formulation in equation 1. The main scope of the design of an efficient level sets segmentation strategy is to devise a relevant external energy term. The standard implementation of the DRLSE framework formulates the external energy term as a combination of two distinct terms:

$$\mathcal{E}_{ext} = \mathcal{L}(\phi) + \mathcal{A}(\phi) \tag{7}$$

where $\mathcal{L}$ is the length term, which when minimized settles the contour at the boundaries of the objects whereas $\mathcal{A}$ is the area term which controls the speed of the active contour. $\mathcal{L}$ can be written as [24]

$$\mathcal{L}(\phi) = \int_{\Omega} g\delta(\phi)|\nabla\phi| d\Omega \tag{8}$$

where δ is the Dirac delta function and g is the edge indicator function given as:

$$g = \frac{1}{1 + |\nabla G_\sigma * I|^2} \tag{9}$$

where G_σ is a Gaussian kernel with standard deviation σ. The first variation of the length term is given by [24]:

$$\frac{\partial\mathcal{L}}{\partial\phi} = \left[\delta(\phi)\nabla.\frac{\nabla\phi}{|\nabla\phi|}g\right] \tag{10}$$

The term $\mathcal{A}(\phi)$ controls the speed of the curve evolution and is composed of two components:

$$\mathcal{A}(\phi) = \mathcal{A}_e + \mathcal{A}_p \tag{11}$$

For $\mathcal{A}_e$, we follow the definition which is similar to that in [23]

$$\mathcal{A}_e = \int_{\Omega} gH(-\phi) d\Omega \tag{12}$$

where $H(\phi)$ is the Heaveside function and g is defined as in equation 9. This term controls the speed of the curve evolution (for details, please see reference [23]) and mainly relies on edges in the images. The first variation of this term can be written as

$$\frac{\partial\mathcal{A}_e}{\partial\phi} = g\delta(\phi) \tag{13}$$

The term $\mathcal{A}_p$ is formulated assuming that an image can be modeled as a mixture of Gaussians which is the main contribution of this paper.

III. GMM BASED BHATTACHARYA FLOW

In this section, we aim to derive an external energy term assuming that an image is modeled as a mixture of Gaussian functions.

A. GAUSSIAN MIXTURE MODEL (GMM)

The GMM is constructed from an image assuming that the groups of pixels in the images can be written as a multivariate Gaussian distribution. For an image segmentation problem, such a mixture for object and background can be written as

$$p(I) = p(I|R_O) + p(I|R_B) \tag{14}$$

where $p(I|R_O)$ and $p(I|R_O)$ can be given by

$$p(I|R_O) \sim \mathcal{N}(\mu_O, \Sigma_O)$$
$$p(I|R_B) \sim \mathcal{N}(\mu_B, \Sigma_B)$$

where μ_O is mean and Σ_O is the variance of the distribution of the object whereas μ_B and Σ_B are the parameters for the background. Generically if the distance between the object and background distributions is maximized using curve evolution, segmentation can be performed. Several metrics can be used for the calculation of this distance [25]. When considering these metrics, it was observed that in most practical cases, the Bhattacharyya metric turns out to give better results as compared to its counterparts [26]. Moreover, another advantage of using this metric is that it has a particularly simple analytic form. Therefore, we use the Bhattacharya distance to measure the difference between two distributions.

B. BHATTACHARYYA BASED DISTANCE

Given that the distributions for the regions inside and outside the contour ϕ are represented as p_O and p_B respectively, the closed form Bhattacharyya distance between two multivariate Gaussian distributions can be written as

$$D_B(p_B, p_O) = \frac{1}{8}\mu^t \Sigma \mu + \frac{1}{2}\ln\left(\frac{\det \Sigma^{-1}}{\sqrt{\det \Sigma_O \det \Sigma_B}}\right) \quad (15)$$

where

$$\mu = \mu_O - \mu_B \quad (16)$$

μ_O and μ_B are the mean of the distributions of the object and background respectively. In the same way, if Σ_O is a variance of the object distribution and Σ_B is a variance of the background distribution, Σ is defined as

$$\Sigma = \left(\frac{\Sigma^O + \Sigma^B}{2}\right)^{-1} \quad (17)$$

The first term in equation 15 calculates the difference between the means μ_O and μ_B weighted by the covariance matrices Σ_O and Σ_B. The second term calculates the difference between the covariance matrices Σ_O and Σ_B only and is not dependant on the means μ_O and μ^B.

C. FORMULATION OF $\mathcal{A}_u$

For the area term, we formulate an optimization problem by simply maximizing the distance between the empirical distributions of the object and the background

$$\mathcal{A}_u(\phi) = \text{argmax}_\phi\{D_B((p(I|R_O))||(p(R_B)))\} \quad (18)$$

where $p(I|R_O)$ is the empirical distribution for the object whereas $p(I|R_B)$ is the empirical distribution of the background, respectively. This maximization can be converted to a minimization problem as follows

$$\mathcal{A}_u(\phi) = -\text{argmin}_\phi\{D_B((p(I|R_O))||(p(R_B)))\} \quad (19)$$

D. GRADIENT FLOW

The proposed external energy functional can be minimized by taking the partial differential of equation 19. Both mixtures pertaining to the object and background are composed of two variables i.e., means and standard deviations. Effectively, the derivative of equation 19 can be written as

$$\frac{\partial \mathcal{A}_u}{\partial \phi} = \frac{\partial \mathcal{A}_u}{\partial \mu} + \frac{\partial \mathcal{A}_u}{\partial \Sigma} \quad (20)$$

where μ and ϕ take definitions from equations 16 and 17 respectively. The partial derivative of $\mathcal{A}_u$ with respect to Σ_O is as follows

$$\begin{aligned}\frac{\partial \mathcal{A}_u}{\partial \Sigma_O} &= \frac{\partial[D_B((p(I|R_O))||(p(R_O)))]}{\partial \Sigma_O}\\ &= \frac{\partial}{\partial \Sigma_O}\left[\frac{1}{8}\mu_O^t \Sigma_O \mu_O + \frac{1}{2}\ln\left(\frac{\det \Sigma_O^{-1}}{\sqrt{\det \Sigma_O \det \Sigma_B}}\right)\right]\end{aligned}$$

Given that the derivation is a linear operator,

$$\begin{aligned}\frac{\partial \mathcal{A}_u}{\partial \Sigma_O} = \frac{\partial}{\partial \Sigma_O}\left[\frac{1}{8}\mu_O^t \Sigma_O \mu_O\right]\\ + \frac{\partial}{\partial \Sigma_O}\left[\frac{1}{2}\ln\left(\frac{\det \Sigma_O^{-1}}{\sqrt{\det \Sigma_O \det \Sigma_B}}\right)\right]\end{aligned}$$

Using equations (72) and (55) from Petersen et al. [27], the above expression can be simplified as follows

$$\frac{\partial \mathcal{A}_u}{\partial \Sigma_O} = \frac{1}{8}\mu_O \mu_O^t + \frac{1}{2}\Sigma_O - \frac{1}{4}\Sigma_O^{-1} \quad (21)$$

Now taking the partial derivative of O with respect to μ_O and using p. 11 (81) from [27], we obtain

$$\frac{\partial \mathcal{A}_u}{\partial \mu_O} = \frac{1}{8}\Sigma_O \mu_O \quad (22)$$

Similarly, we can conclude that

$$\frac{\partial \mathcal{A}_u}{\partial \Sigma_B} = \frac{1}{8}\mu_B \mu_B^t + \frac{1}{2}\Sigma_B - \frac{1}{4}\Sigma_B^{-1} \quad (23)$$

and

$$\frac{\partial \mathcal{A}_u}{\partial \mu_B} = \frac{1}{8}\Sigma_B \mu_B \quad (24)$$

Substituting these results in equation 20, we obtain

$$\begin{aligned}\frac{\partial \mathcal{A}_u}{\partial \phi} = \frac{1}{8}\mu_O \mu_O^t + \frac{1}{2}\Sigma_O - \frac{1}{4}\Sigma_O^{-1} + \frac{1}{8}\Sigma_O \mu_O + \frac{1}{8}\mu_B \mu_B^t\\ + \frac{1}{2}\Sigma_B - \frac{1}{4}\Sigma_B^{-1} + \frac{1}{8}\Sigma_B \mu_B \quad (25)\end{aligned}$$

The overall optimization function is obtained by substituting $\partial \mathcal{A}_p / \partial \phi$ into Eq. 6

$$\begin{aligned}\frac{\partial \mathcal{J}}{\partial \phi} = -\gamma\left[\Delta\phi - \nabla.\frac{\nabla\phi}{|\nabla\phi|}\right] - \lambda\left[\delta(\phi)\nabla.\frac{\nabla\phi}{|\nabla\phi|}g\right] - g\delta(\phi)\\ + \left[\frac{1}{8}\mu_O \mu_O^t + \frac{1}{2}\Sigma_O + \frac{1}{8}\Sigma_O \mu_O - \frac{1}{4}\Sigma_O^{-1} + \frac{1}{8}\mu_B \mu_B^t\right.\\ \left. + \frac{1}{2}\Sigma_B + \frac{1}{8}\Sigma_B \mu_B - \frac{1}{4}\Sigma_B^{-1}\right] \quad (26)\end{aligned}$$

The third term in equation 26 is based on region based terms (object and background distributions) and exhibits the most fundamental difference of the proposed method from DRLSE [23].

IV. ACTIVE CONTOURS IMPLEMENTATION

The time dependent evolution function $\phi(x, y, t)$ is a 2D function for which the spatial derivatives $\partial\phi/\partial x$ and $\partial\phi/\partial y$ are approximated using the finite differences scheme [23]. Fixed space steps of $\Delta x = \Delta y = 1$ are considered to compute spatial derivatives. Given that a time dependent function $\phi(x, y, t)$ can be written as $\phi^k_{i,j}$, the level set evolution equation can be discretized as $(\phi^{k+1}_{i,j} - \phi^k_{i,j})/\Delta t = L^k_{i,j}$ where $L^k_{i,j}$ is obtained as an approximation of the right hand side of the evolution equation (eq. 26). The iterative scheme to update the level sets function can be written as:

$$\phi^{k+1}_{i,j} = \phi^k_{i,j} + \Delta t L^k_{i,j} \tag{27}$$

which is an iterative process of curve evolution and can be used for numerically implementing the proposed framework. The steps involved in the curve evolution algorithm are as follows:

1) The zero level contour is initially constructed by initialization of ϕ at $t = 0$ such that the region lying inside ϕ is considered as an object while that lying outside ϕ is considered as background.
2) The histogram-based features are obtained for both the object and background for calculating the term A_p.
3) Assuming a specific time step Δt, we calculate $\phi^{k+1}_{i,j}$ using equation 27 which yields the new curve.
4) The steps (2) and (3) are repetitively performed until curve evolution stops or its speed becomes very small. The speed of curve evolution will slow down as the curve settles at the object boundaries since that will lead to the solution of the optimization problem.

A. ASSUMPTIONS AND LIMITATIONS

The proposed model for segmentation using active contours is based on modeling the object and the background using the Gaussian mixture models followed by a gradient flow for which the closed-form solution exists. However before we proceed to calculate the gradient flow, the statistical assumptions encompassing the solution should be underlined. Firstly for the two distinct regions that have to be segmented, the samples of $I(x, y)$ can be characterized by two conditional density functions $p(I|R_O)$ and $p(I|R_B)$ which describe the probability distribution of a specific feature in the images for the object and background respectively. For the calculation of these distributions, we have used the EM algorithm [28] assuming that the object and the background distributions are mutually independently and identically distributed (i.i.d). This assumption has an obvious disadvantage that it is not possible to take into consideration the dependency structure between the samples of $I(x, y)$. This assumption is mainly meant to simplify the implementation of the optimization algorithm. Taking into account this dependency can be done using, for example, the theory of Markov fields [29] that could rather improve the precision of the algorithm. However, such rigorous mathematical modeling will induce a very high computational cost to the overall segmentation process and will not add significant value to the output of the algorithm.

B. SELECTED IMAGE FEATURES

There could be a wide range of possibilities as far as the nature of image features is concerned. The methodology is based on convex optimization between two density functions. Therefore, the histogram-based features can be used in this implementation. Given that we have an image $I(x, y) : \Omega \rightarrow \mathbb{R}$ to a vector-valued variable $J(x) : \Omega \rightarrow \mathbb{R}^N$, which is an N- dimensional feature that is obtained as a result of a transformation $\mathcal{W}$ such that $J(x) = \mathcal{W}\{I(x, y)\}$. In the current implementation, the histogram of gray levels of $I(x, y)$ is used for calculating the density function for segmentation purposes given that this choice has proven to be successful in various practical settings [30], [31]. Therefore, any color image belonging to any imaging modality is first converted to its gray scale counterpart. This is followed by the selection of an initial contour, based on which the object (inner part of the initial contour) and background (area lying outside the initial contour) distributions are created using the EM algorithm. The contour is later evolved, and the updated distributions are estimated to lead to the proposed optimization. Flow diagram of the proposed method is shown in Fig. 2 along with the implementation of the iterative algorithm with progressive curve evolution (Fig. 1).

V. EXPERIMENTAL RESULTS

Since the proposed segmentation method incorporates a statistical framework in addition to the use of edge features, our main aim for the experiments is to show the generalization capability of the segmentation method. Therefore, instead of focusing on a specific imaging scenario, we have performed our experiments on images that come from radically different imaging modalities. Accordingly, our aim is not to claim that we obtain the best results for a specific (or all) imaging modality but to do a broader analysis of the proposed method. In this section, two distinct experiments are performed. In the first experiment, we demonstrate the proposed concept by using the segmentation method for segmenting medical images from two distinct imaging modalities: Computed Tomography (CT) and Ultrasound (US). Later, we perform experiments on an open dataset from three radically different imaging modalities: Magnetic Resonance Imaging (MRI), Dermoscopy and Chromoendoscopy. For these datasets, the manual annotations done by experts are available. The proposed methods are evaluated using the Dice similarity coefficient [32]. We have compared the segmentation results of the proposed method with Li's distance regularized level sets (DRLSE) [23], the Chen-Vese implementation (C-V) [33] and the Kullback-Leibler based level sets (KL-LS) [34].

Regularization and length terms are implemented using Li's method [24]. A Gaussian mixture of *gray level distributions* is used for object and background (differentiated by ϕ). As ϕ evolves, the GMM parameters start to change

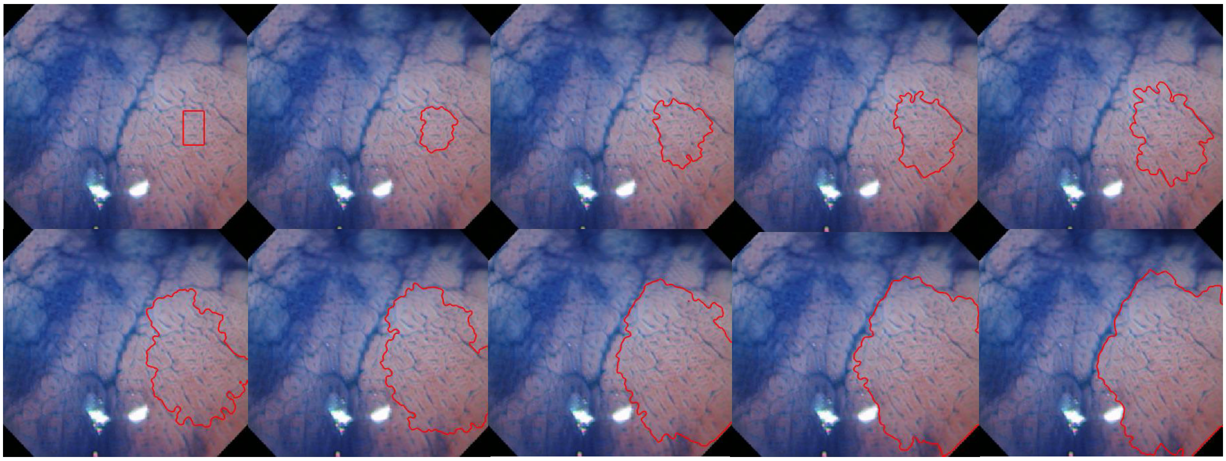

FIGURE 1. Results of iterative implementation of segmentation algorithm after every 20 steps.

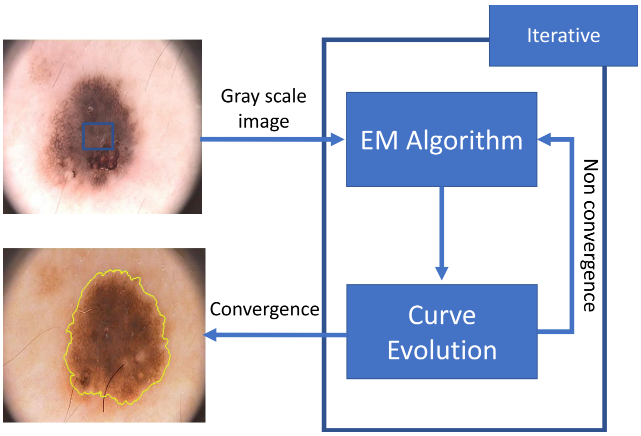

FIGURE 2. Flow diagram showing the implementation of the iterative framework for performing curve evolution.

until they converge to some specific values. The resulting ϕ is the contour that differentiates between the object and background. The proposed method is implemented in Matlab and utilizes the DRLSE implementation model with the same parameter values as used by Li et al. [23]. For all images, a small square at the center of the lesion is taken as an initial contour which is subjected to evolution. The curve evolution is stopped if the curve does not evolve during 5 consecutive iterations or the number of iterations exceeds a specific count.

A. PROOF OF CONCEPT

We have used three images each from two distinct imaging modalities: computed tomography (CT) and ultrasound (US). We have two CT images from the liver and one image from the brain for segmenting lesions in the respective organs. Among ultrasound images, we have used one image each from ovarian, abdominal and renal scans of the patients. This is a diverse dataset given that the images are based on two distinct technologies i.e., x-rays and acoustics which exhibit distinct visual characteristics.

We will focus our attention to two main aspects: 1). Noise robustness, and 2). Weak edge preservation. The DRLSE method is highly reliant on the object boundaries which are typically weak in medical imaging (Fig. 3 and 4). Consequently, the leaking of active contours across the object boundaries takes place very often. In the case of CT images (Fig. 3) the lesion boundaries are weak resulting in lack of convergence of DRLSE. In ultrasound images (Fig. 4) there is a lot of speckle-noise due to which the contours leak across the lesions. Due to higher sensitivity to noise, the formation of small contours inside the segmented lesions also takes place. The overall segmentation results for DRLSE are better in

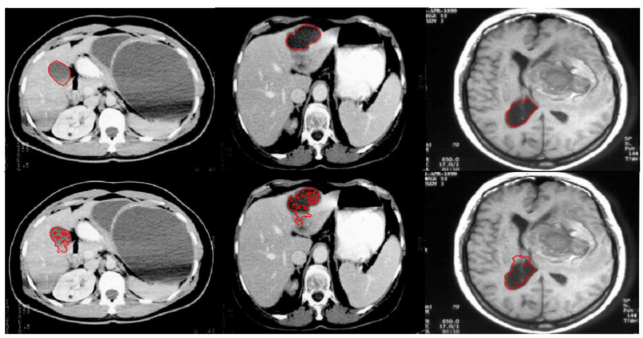

FIGURE 3. CT images: First row shows implementation of our method, the second row shows DRLSE.

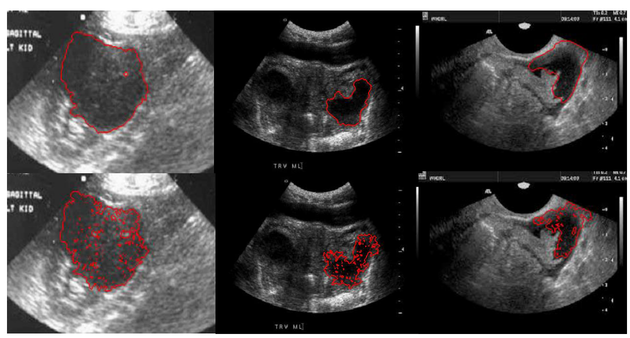

FIGURE 4. Ultrasound images: The first row shows implementation of our method, the second row shows DRLSE.

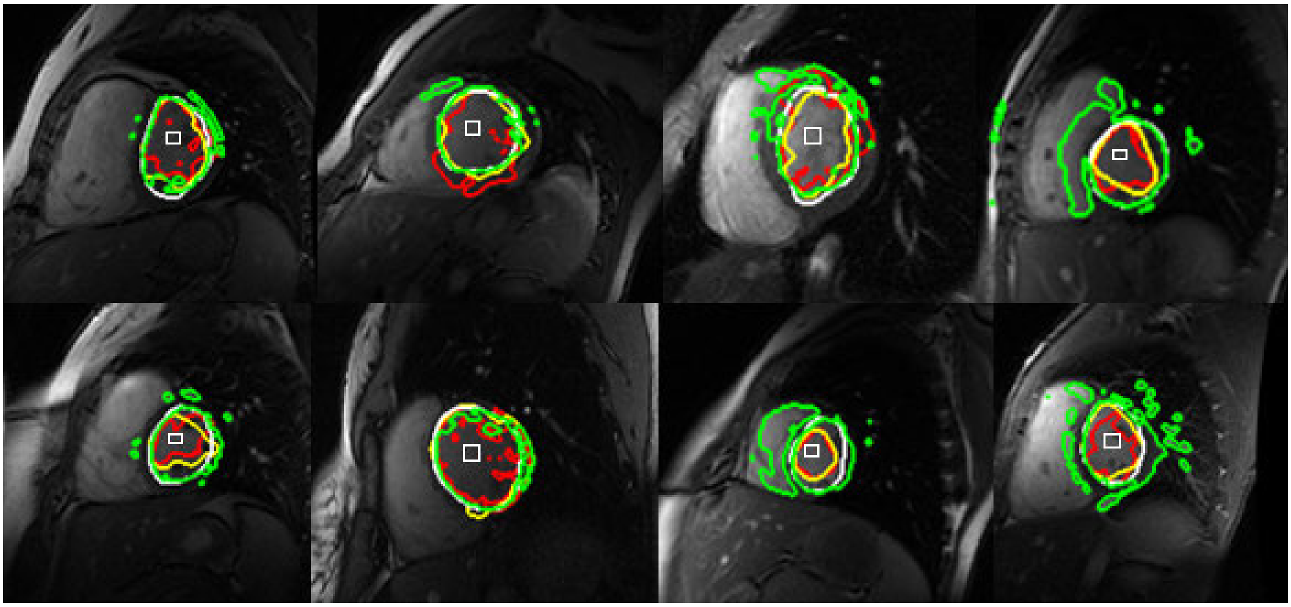

FIGURE 5. Segmentation of MRI images using manual annotations (white), DRLSE implementation (red), C-V region based active contours model (green) and the proposed implementation (yellow). The curves are initialized with a small rectangle in the centre of the left ventricle.

the case of dermoscopy (Fig. 7) due to a relatively higher contrast but the formation of small segments is most dominant due to the higher texture (hair, vessels etc.) in the images. The C-V method performs curve evolution without edges and converges conservatively. The curve evolution does not encapsulate the true boundaries of the objects that can potentially lead to imprecise measurements of the objects in the case of ultrasound and CT images [35], [36]. The proposed method shows good segmentation results in comparison to its counterparts and its strength lies in its complementary nature: the edge term uses local curvature-based features for curve evolution whereas the area term penalizes it by relying on the region based characteristics of the images. This allows the proposed method to generalize well to radically different imaging modalities.

Next, to quantitatively assess the proposed method, we need to make a selection of the relevant datasets. Since method is based on initially modelling an image as a GMM of the object and the background, a well suited imaging modality should conform to the underlying assumption. In this context, Dermoscopy and Gastroenterology are two imaging modalities which are quite suitable to evaluate the performance of the proposed method. In contrast to these, we have chosen another imaging modality (MRI) in which the conformity of the data strongly to the GMM based modeling is not applicable. This combination of three imaging modalities is complementary and thus can help us in fairly assessing the performance of the proposed method.

B. SEGMENTATION OF MRI IMAGES

Our next set of experiments were performed on short-axis cardiac [1]MRI image sequences acquired from 33 subjects.

[1]http://www.cse.yorku.ca/ mridataset/

Most of the images displayed a variety of abnormalities including cardiomyopathy, aortic regurgitation and enlarged ventricle. All subjects were under the age of 18 years. The dataset is publicly available for research purposes (details about the data can be obtained from the webpage). The Gaussian mixture is constructed from the gray level distribution of the images. The segmentation algorithms are initialized with a small region in the center of the left ventricle and the curves are subjected to evolve outwards until the endocardial contour is encapsulated. The results are compared with the manual annotations using two measures: the Dice similarity coefficient (DSC) and Jaccard index (JI). If A is the manual annotation and S is the segmented region, the DSC between A and S can be represented as

$$DSC = 2\frac{A \cap S}{A + S} \tag{28}$$

The DSC values range between 0 and 1 for no overlap and identical contours, respectively, for annotated and segmented regions. Similarly, the JI can be represented as follows

$$JI = \frac{A \cap S}{A \cup S} \tag{29}$$

Again the JI values range between 0 and 1 for no overlap and identical contours, respectively. Our results demonstrate that the proposed method shows very good performance in segmenting MRI images with a DSC of 0.77 and JI of 0.63. Visual inspection of the segmentation results (Fig. 5) qualitatively validates the findings given that the proposed method shows good segmentation results in comparison to the manual annotations. The proposed method also outperforms the other methods that have been considered in this paper. The main difference in performance comes from two important factors: The epi- and endocardial boundaries in the image exhibit weaker boundaries and the DRLSE and C-V methods result

TABLE 1. Segmentation results obtained for MRI images using average dice similarity coefficient.

Methods	DSC	JI
Proposed	0.77	0.63
KL-LS	**0.79**	**0.65**
DRLSE	0.74	0.59
C-V	0.75	0.60

in leaking of the contours due to weaker edges (e.g., Fig. 5: col 4). Secondly, the DRLSE and C-V implementations are unable to incorporate the papillary tissues within the segmenting contour resulting in imperfection in some images. In such cases, the papillary muscles are considered as part of the myocardium whereas the algorithm excludes it from the segmentation resulting in segmentation errors. When the region based term is used, the segmentation results improve giving better quantitative measurements. In summary, we conclude that adding an area based term to the existing edge-based DRLSE implementation improves the segmentation results. The KL-LS method shows the best results with a DSC of 0.79 and JI of 0.65. The proposed method performs about 2% lower than that of KL-LS. We attribute this lower performance of the proposed method to the fact that by definition, the assumption of an image being modeled as GMMs with distinct Gaussians for both the object and background does not precisely apply to this scenario, thus leading to the imperfections in the segmentations.

C. SEGMENTATION OF DERMOSCOPY IMAGES

Our next set of experiments were performed on dermoscopy images. This selection of the imaging modality is complementary in nature as compared to MRI imaging given that they are obtained from a dermoscopy, which uses white light for the illumination of the skin tissues for visual inspection. The dataset that we have used for our experiments was acquired from the Hospital Pedro Hispano, Matosinhos [37]. The dataset is composed of 200 dermoscopic images which have been annotated (for identifying skin lesions) by experts. The dataset along with its annotations have been made publicly available. We perform automatic segmentation of dermoscopy images and compare them to the manual annotations (available publicly) quantitatively using the DSC and JI.

Good results are obtained using the proposed method (Table. 2). When DRLSE is used, a relatively lower DSC and JI are observed. We attribute the low performance to the fact that it uses the edges of images which exhibit a weak distinction between the lesion and the background for some images (e.g. Fig. 7 row one column one, row one column two, row one column three). In the former, there is excessive hair in the image which causes leakage of the active contour whereas, in the last case, the lesion has weaker edges leading to leaking of the active contour. When the region-based term is integrated in the segmentation framework, better segmentation results are obtained and we get a high Dice coefficient. The C-V model also shows lower performance, which is also attributed to the lack of clear boundaries between the lesion and the background. The active contour exceeds the desired boundaries in these cases, giving rise to erroneous segmentation. With the addition of the region based term, we obtain a DSC of 0.84 and JI of 0.72. Given this, our experimental results are consistent with those obtained for the MRI images in that the addition of area terms in the segmentation framework improves the segmentation results. The proposed method also outperforms KL-LS in contrast to the results on the MRI imaging modality due to the fact that the GMM based model fits well into the dermoscopy imaging scenario.

TABLE 2. Segmentation results obtained for dermoscopy images using average dice similarity coefficient.

Methods	DSC	JI
Proposed	**0.84**	**0.72**
KL-LS	0.82	0.69
DRLSE	0.82	0.69
C-V	0.81	0.68

D. SEGMENTATION OF GASTROENTEROLOGY IMAGES

Our next set of experiments were performed on chromoendoscopy (CH) images. Specifically, we have done experiments on the vital stained magnification endoscopy images. This is a very different imaging modality in which the images of the upper gastrointestinal tract are stained using a dying agent such as methylene blue followed by the visual inspection of the tissue under observation for finding gastric lesions. The inspection of the tissue is typically done using an endoscope which has a camera attached to its tip that uses white light to illuminate the tissue. The dataset is composed of 176 images, which have been acquired during live endoscopic examinations given their clinical relevance (details about the dataset can be obtained from [38]). We perform automatic segmentation of CH images and compare the results with the manual annotations using the DSC and JI.

The most significant difference of CH images from the other imaging modalities that have been considered in this paper is that the CH images have a very high texture. This makes this segmentation problem very challenging as the presence of high texture signifies the visual patterns which are relevant for clinical evaluation of the images. Effectively, all the methods which are based on edges are not expected to perform well. The C-V model does not work well on images with intensity inhomogeneities, which is a very common scenario in CH images after the tissues are stained with methylene blue. This results in the inferior performance obtained by the C-V method resulting in the formation of small segments in areas having intensity inhomogeneities. The DRLSE method is based on the edge indicator function which does not show good performance either. This is attributed to the rich texture in the images, resulting in convergence issues. The experimental results are consistent for the CH images and the other two imaging modalities given that the proposed method

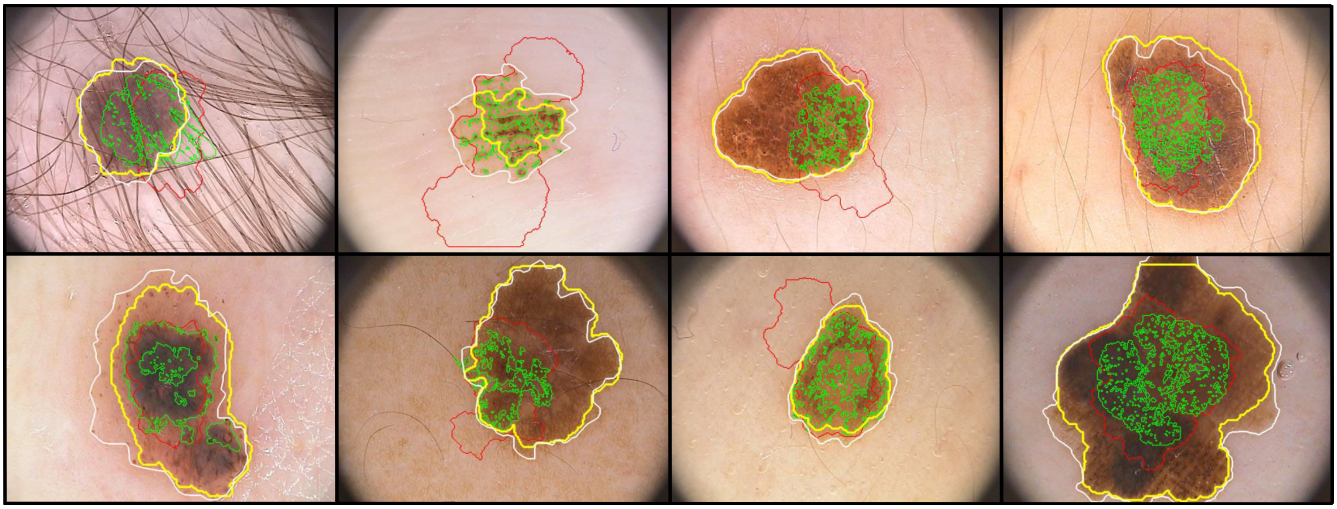

FIGURE 6. Segmentation of Dermoscopy images using Manual annotations (white), DRLSE implementation (red), C-V region based active contours model (green) and the proposed implementation (yellow). The curves are initialized with a small rectangle in the centre of the skin lesions.

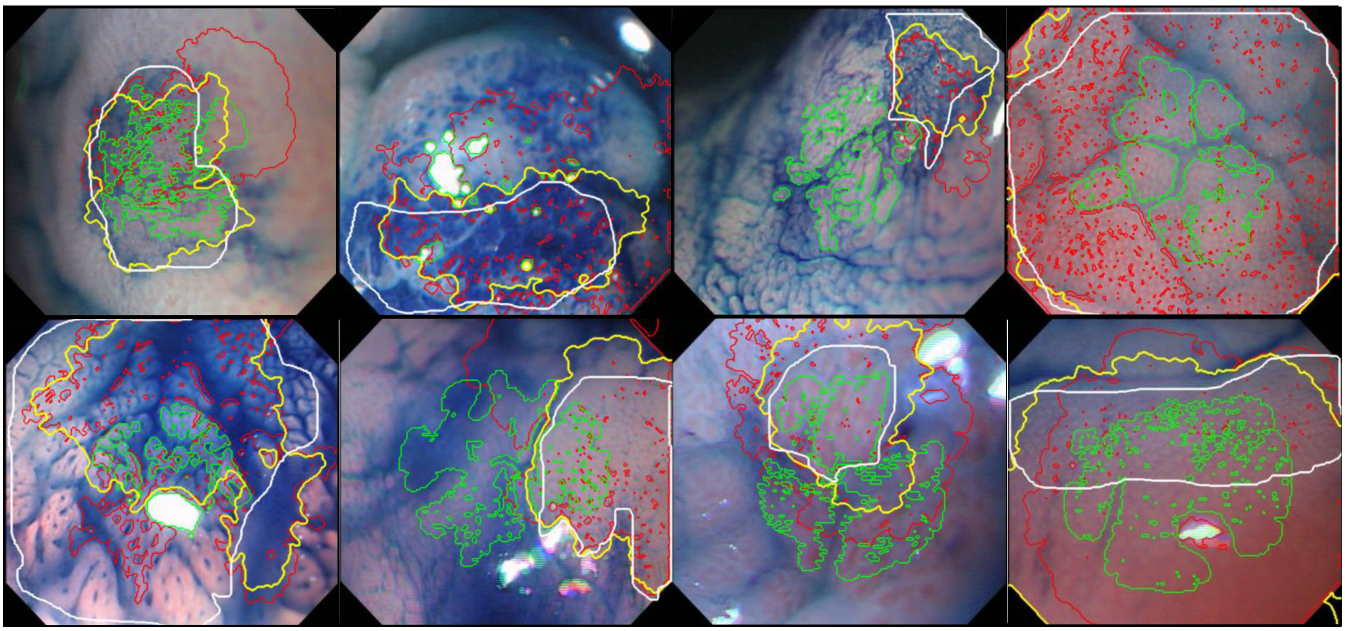

FIGURE 7. Segmentation of CH images using manual annotations (white), DRLSE implementation (red), C-V region based active contours model (green) and the proposed implementation (yellow). The curves are initialized with a small rectangle in the centre of the gastric lesions.

TABLE 3. Segmentation results obtained for CH images using average dice similarity coefficient.

Methods	DSC	JI
Proposed	**0.73**	**0.57**
KL-LS	0.70	0.54
DRLSE	0.66	0.49
C-V	0.63	0.46

outperforms the other methods that have been considered in this paper with the most significant impact on the results made by the addition of region-based information to the DRLSE method. The proposed method also performs better than KL-LS given that the modeling of an image as GMMs often applies to Gastroenterology images.

VI. CONCLUSION

In this paper, we have proposed a novel framework to segment objects in medical images with poorly defined boundaries. The variational level sets framework is extended to incorporate a novel term which maximizes the distance between the object and background distributions using the Bhattacharya distance. The proposed method is complementary given that it is composed of an edge term, that relies on the edges of the objects, and an area term that takes the probability distributions of the objects and background into account. To validate the effectiveness of the algorithm, we have first performed a proof of concept on ultrasound and computed tomography images. Comprehensive experiments have been performed on images from three distinct imaging modalities i.e., magnetic resonance images, dermoscopy and chromoendoscopy images. Our results show that the proposed method performs well for these imaging modalities, both qualitatively and quantitatively.

REFERENCES

[1] G. Aubert and P. Kornprobst, *Mathematical Problems in Image Processing: Partial Differential Equations and the Calculus of Variations*, vol. 147. New York, NY, USA: Springer-Verlag, 2006.

[2] M. Kass, A. Witkin, and D. Terzopoulos, "Snakes: Active contour models," *Int. J. Comput. Vis.*, vol. 1, no. 4, pp. 321–331, Jan. 1988.

[3] S. Osher and J. A. Sethian, "Fronts propagating with curvature-dependent speed: Algorithms based on Hamilton-Jacobi formulations," *J. Comput. Phys.*, vol. 79, no. 1, pp. 12–49, Nov. 1988.

[4] V. Caselles, F. Catté, T. Coll, and F. Dibos, "A geometric model for active contours in image processing," *Numer. Math.*, vol. 66, no. 1, pp. 1–31, Dec. 1993.

[5] V. Caselles, R. Kimmel, and G. Sapiro, "Geodesic active contours," in *Proc. Int. J. Comput. Vis.*, vol. 22, no. 1, pp. 61–79, 1997.

[6] X. Du and T. D. Bui, "A new model for image segmentation," *IEEE Signal Process. Lett.*, vol. 15, no. 1, pp. 182–185, Jan. 2008.

[7] S. Mahmoodi, "Shape-based active contours for fast video segmentation," *IEEE Signal Process. Lett.*, vol. 16, no. 10, pp. 857–860, Oct. 2009.

[8] J. Melonakos, E. Pichon, S. Angenent, and A. Tannenbaum, "Finsler active contours," *IEEE Trans. Pattern Anal. Mach. Intell.*, vol. 30, no. 3, pp. 412–423, Mar. 2008.

[9] R. Kimmel, "Fast edge integration," in *Geometric Level Set Methods in Imaging, Vision, and Graphics*. New York, NY, USA: Springer, Apr. 2006, pp. 59–77.

[10] F. Riaz, A. Hassan, and J. Zeb, "Distance regularized curve evolution: A formulation using creaseness features for dermoscopic image segmentation," in *Proc. 12th Int. Conf. Signal Process. (ICSP)*, Oct. 2014, pp. 1061–1065.

[11] A. Belaid, D. Boukerroui, Y. Maingourd, and J.-F. Lerallut, "Phase-based level set segmentation of ultrasound images," *IEEE Trans. Inf. Technol. Biomed.*, vol. 15, no. 1, pp. 138–147, Jan. 2011.

[12] Q. Abbas, M. Celebi, and I. F. García, "Hair removal methods: A comparative study for dermoscopy images," *Biomed. Signal Process. Control*, vol. 6, no. 4, pp. 395–404, Oct. 2011.

[13] X. Yuan, N. Situ, and G. Zouridakis, "A narrow band graph partitioning method for skin lesion segmentation," *Pattern Recognit.*, vol. 42, no. 6, pp. 1017–1028, Jun. 2009.

[14] F. Riaz, F. B. Silva, M. D. Ribeiro, and M. T. Coimbra, "Impact of visual features on the segmentation of gastroenterology images using normalized cuts," *IEEE Trans. Biomed. Eng.*, vol. 60, no. 5, pp. 1191–1201, May 2013.

[15] Z. Ji, Y. Xia, Q. Sun, G. Cao, and Q. Chen, "Active contours driven by local likelihood image fitting energy for image segmentation," *Inf. Sci.*, vol. 301, pp. 285–304, Apr. 2015.

[16] Y. Zhou, W.-R. Shi, W. Chen, Y.-L. Chen, Y. Li, L.-W. Tan, and D.-Q. Chen, "Active contours driven by localizing region and edge-based intensity fitting energy with application to segmentation of the left ventricle in cardiac CT images," *Neurocomputing*, vol. 156, pp. 199–210, May 2015.

[17] T. Chan and L. Vese, *An Active Contour Model Without Edges* (Lecture Notes in Computer Science). Berlin, Germany: Springer, 1999.

[18] A. Khadidos, V. Sanchez, and C.-T. Li, "Weighted level set evolution based on local edge features for medical image segmentation," *IEEE Trans. Image Process.*, vol. 26, no. 4, pp. 1979–1991, Apr. 2017.

[19] V. Estellers, D. Zosso, X. Bresson, and J.-P. Thiran, "Harmonic active contours," *IEEE Trans. Image Process.*, vol. 23, no. 1, pp. 69–82, Jan. 2014.

[20] K. Zhang, L. Zhang, H. Song, and D. Zhang, "Reinitialization-free level set evolution via reaction diffusion," *IEEE Trans. Image Process.*, vol. 22, no. 1, pp. 258–271, Jan. 2013.

[21] L. Jin-qing and L. Wei-Wei, "Adaptive medical image segmentation algorithm combined with DRLSE model," *Procedia Eng.*, vol. 15, pp. 2634–2638, 2011.

[22] N. Jafarian, K. Kazemi, H. A. Moghaddam, R. Grebe, M. Fournier, M. S. Helfroush, C. Gondry-Jouet, and F. Wallois, "Automatic segmentation of newborns' skull and fontanel from CT data using model-based variational level set," *Signal, Image Video Process.*, vol. 8, no. 2, pp. 377–387, 2014.

[23] C. Li, C. Xu, C. Gui, and M. D. Fox, "Distance regularized level set evolution and its application to image segmentation," *IEEE Trans. Image Process.*, vol. 19, no. 12, pp. 3243–3254, Dec. 2010.

[24] C. Li, C. Xu, C. Gui, and M. Fox, "Level set evolution without re-initialization: A new variational formulation," in *Proc. IEEE Comput. Soc. Conf. Comput. Vis. Pattern Recognit. (CVPR)*, vol. 1, Jul. 2005, pp. 430–436.

[25] T. M. Cover and J. A. Thomas, *Elements of Information Theory*. Hoboken, NJ, USA: Wiley, 2012.

[26] T. Kailath, "The divergence and Bhattacharyya distance measures in signal selection," *IEEE Trans. Commun.*, vol. 15, no. 1, pp. 52–60, Feb. 1967.

[27] K. B. Petersen and M. S. Pedersen, "The matrix cookbook," *Tech. Univ. Denmark*, vol. 7, no. 15, p. 510, 2008.

[28] T. K. Moon, "The expectation-maximization algorithm," *IEEE Signal Process. Mag.*, vol. 13, no. 6, pp. 47–60, Nov. 1996.

[29] E. Vanmarcke, *Random Fields, Analysis and Synthesis*. Singapore: World Scientific, 2010.

[30] M. Yuksel and M. Borlu, "Accurate segmentation of dermoscopic images by image thresholding based on type-2 fuzzy logic," *IEEE Trans. Fuzzy Syst.*, vol. 17, no. 4, pp. 976–982, Aug. 2009.

[31] Y. Xia, Z. Ji, and Y. Zhang, "Brain MRI image segmentation based on learning local variational Gaussian mixture models," *Neurocomputing*, vol. 204, pp. 189–197, Sep. 2016.

[32] C. J. V. Rijsbergen, *Information Retrieval*. Newton, MA, USA: Butterworth-Heinemann, 1979.

[33] T. Chan and L. Vese, "Active contours without edges," *IEEE Trans. Image Process.*, vol. 10, no. 2, pp. 266–277, Feb. 2001.

[34] F. Riaz, S. Naeem, R. Nawaz, and M. Coimbra, "Active contours based segmentation and lesion periphery analysis for characterization of skin lesions in dermoscopy images," *IEEE J. Biomed. Health Inform.*, vol. 23, no. 2, pp. 489–500, Mar. 2019.

[35] M. Gundappa, S. Y. Ng, and E. J. Whaites, "Comparison of ultrasound, digital and conventional radiography in differentiating periapical lesions," *Dentomaxillofacial Radiol.*, vol. 35, no. 5, pp. 326–333, 2006.

[36] I. Rauscher, M. Eiber, S. Furst, M. Souvatzoglou, S. G. Nekolla, S. I. Ziegler, E. J. Rummeny, M. Schwaiger, and A. J. Beer, "PET/MR imaging in the detection and characterization of pulmonary lesions: Technical and diagnostic evaluation in comparison to PET/CT," *J. Nucl. Med.*, vol. 55, no. 5, pp. 724–729, May 2014.

[37] T. Mendonca, P. M. Ferreira, J. S. Marques, A. R. S. Marcal, and J. Rozeira, "PH2–A dermoscopic image database for research and benchmarking," in *Proc. 35th Annu. Int. Conf. IEEE Eng. Med. Biol. Soc. (EMBC)*, Jul. 2013, pp. 5437–5440.

[38] F. Riaz, F. B. Silva, M. D. Ribeiro, and M. T. Coimbra, "Invariant Gabor texture descriptors for classification of gastroenterology images," *IEEE Trans. Biomed. Eng.*, vol. 59, no. 10, pp. 2893–2904, Oct. 2012.

FARHAN RIAZ received the B.E. degree from the National University of Sciences and Technology (NUST), Islamabad, Pakistan, the M.S. degree from the Technical University of Munich, Germany, and the Ph.D. degree from the University of Porto, Portugal. Since 2012, he has been an Assistant Professor with NUST. His research interests include biomedical signal and image processing, applied machine learning, and computer vision.

SAAD REHMAN received the M.S. and Ph.D. degrees from the University of Sussex, Brighton, U.K. He is currently an Associate Professor with the College of Electrical and Mechanical Engineering, National University of Sciences and Technology, Islamabad. His research interests include correlation pattern recognition, and image and signal processing.

MUHAMMAD AJMAL received the Ph.D. degree in electrical and computer engineering from the University of Porto, Portugal. He is currently serving as a Lecturer in cyber security with the Department of Computer Science and Mathematics, University of Derby. He is currently researching on topics related to privacy-aware collaboration among service providers, secure reputation systems, collaborative security, telephone and next-generation network security, and spam detection.

REHAN HAFIZ received the Ph.D. degree in EE from the University of Manchester, U.K., in 2008. He is currently with Information Technology University (ITU), Lahore, as an Associate Professor of EE. Earlier, he has served as an Assistant Professor with the School of Electrical Engineering and Computer Science, National University of Sciences and Technology, from 2008 to 2015. He founded and directed the Vision Image and Signal Processing (VISpro) Lab that focuses on vision system design, development of power efficient architectures, design of approximate computing-based hardware accelerators, FPGA based designs, multiprojector and immersive display technologies, and applied image and video processing. He holds several patents in U.S., South Korean, and Pakistan patent office. He has published several articles related to custom processor design, application specific processor designing, video stabilization, multiprojector rendering, and approximate computing.

ALI HASSAN received the B.E. and M.S. degrees in computer engineering from the National University of Sciences and Technology (NUST), Pakistan, and the Ph.D. degree from the University of Southampton, U.K., in 2012. He is currently an Assistant Professor with the College of Electrical and Mechanical Engineering, NUST. His research interests include application of machine learning to image processing in the domains of texture classification and biomedical signal processing.

NAIF RADI ALJOHANI received the Ph.D. degree from the University of Southhampton, U.K. He is currently serving as an Associate Professor with the Information Systems Department, Faculty of Computing and Information Technology, King Abdul Aziz University Jeddah, Saudi Arabia. His research interests include social networks, data mining, data science, and linked open data.

RAHEEL NAWAZ served in various senior leadership positions in the private Higher and Further Education Sector; and was an Army Officer before that. He is currently the Director of the Digital Technology Solutions and a Reader in Analytics and Digital Education with Manchester Metropolitan University (MMU). He has founded and/or headed several research units specializing in artificial intelligence, digital transformations, data science, digital education, and apprenticeships in higher education. He has led on numerous funded research projects in the U.K., EU, South Asia, and Middle East. He holds adjunct or honorary positions with several research, higher education, and policy organizations, both in the U.K. and overseas. He regularly makes media appearances and speaks on a range of topics, including digital technologies, artificial intelligence, digital literacy, and higher education.

RUPERT YOUNG received the Ph.D. degree from Glasgow University. Since 1995, he has been with the Department of Engineering and Design, University of Sussex, in which he served as the Head of Department, from 2006 to 2011, where he is currently a Reader. His research interests include computer vision and image processing, pattern recognition, and genetic algorithms.

MIGUEL COIMBRA is one of the founders and the current Director of IT Porto, in which he founded and coordinates the Interactive Multimedia Group, personally leading a team of researchers, including several post docs, Ph.D., M.Sc., and B.Sc. students. He is the current Chair of the Portugal Chapter of the IEEE Engineering and Medicine Society, the former Director of the Master in medical informatics of the University of Porto, and is the Co-Founder of IS4H—Interactive Systems for Healthcare, a spin-off company of the University of Porto, which has licensed and is selling products based on all the interactive auscultation technologies developed by his team. He leads and participates in various projects involving engineering and medicine, namely cardiology and gastroenterology, with current and past cooperations with hospitals in Portugal, Brazil (Pernambuco, Paraíba, Minas Gerais, São Paulo), Germany, and Sweden.